Supplement of Biogeosciences, 22, 5591–5605, 2025 https://doi.org/10.5194/bg-22-5591-2025-supplement © Author(s) 2025. CC BY 4.0 License.





#### Supplement of

Mercury contamination in staple crops impacted by artisanal and small-scale gold mining (ASGM): stable Hg isotopes demonstrate dominance of atmospheric uptake pathway for Hg in crops

Excellent O. Eboigbe et al.

Correspondence to: David S. McLagan (david.mclagan@queensu.ca)

The copyright of individual parts of the supplement might differ from the article licence.

#### **Table of Contents**

S1. Mining activities in Uke ASGM mine and processing sites	2
S2. Maps, images, and details of sampling procedures and sampling sites	
S3. Analytical Methods and Recoveries for CRMs	6
S4. Equations for Two endmember mixing model	10
S5. Method for estimation of annual GEM/Hg(0) dry deposition rates to crops	11
S6. Method for estimation probable dietary intake values	13
S7. THg and stable isotope full results for all samples	14
S8. Pyrolytic Thermal Desorption (PTD) curves for Farm1 and Processing Site (PS) solid-phase speciation/fractionation analyses	20
References (used in Supplementary Information)	22

## S1. Mining activities in Uke ASGM mine and processing sites

Mining involves rudimentary techniques where gold ore is extracted from underground shafts before being transported to the processing site for gold extraction. At the processing site, the ore is crushed into cobbles by hand, primarily by women using hand hammers. The crushed ore is then ground using a hammer mill. To concentrate the gold, the ground ore is processed in a sluice box over a fibrous carpet. Hg is used to amalgamate with the gold particles, and the amalgam is subsequently heated over a fire to volatilize Hg, leaving behind a "sponge gold" (Davies, 2023; Odukoya et al., 2022; Yoshimura et al., 2021).

The town of Uke now has an estimated population of around 20,000, with agriculture and mining as the primary occupations. Major crops cultivated include cassava, maize, peanut (referred to as groundnut in Nigeria), and cowpea. The ASGM processing site is adjacent to the Uke River, which provides water for the local population, and both the agricultural and mining sectors in the area.



Figure S1: The underground mine site where hard rock gold ore is extracted. Extracted ore is transported to nearby processing sites for Hg amalgamation and gold recovery.



Figure S2: Processing of gold ore at the ASGM Processing Site (PS) in Uke. Activities involve crushing and grinding ore, addition of Hg for amalgamation, and burning off the amalgam.

# S2. Maps, images, and details of sampling procedures and sampling sites

#### Details on soil sampling:

Soil samples were stored and sealed in (double) Ziplock bags and transported (at room temperature) the day after collection to the University of Lagos lab and refrigerated for two days at 4 °C before drying. Sample drying was undertaken at the University of Lagos via oven drying until constant weight at ≈35 to 40 °C within 72 hours of sampling to minimize potential losses of Hg. The dried samples were then shipped to Queen's University in Canada for analyses. Aliquots of the PS soil samples were removed before drying and kept as "fresh" (undried) samples for Hg speciation analysis to minimize losses of any Hg(0) that might be present in soils. Nonetheless, we note that much of any Hg(0) present in these "fresh" samples still may have been lost during shipment and storage before analysis, a process that is difficult to prevent (Hojdová et al., 2015; Reis et al., 2015, McLagan et al., 2022b).

#### MerPAS GEM (air) sampling:



Figure S3: Deployment of MerPAS at Uke ASGM processing site.

After deployment, MerPAS were sealed with storage caps and the seal triple-wrapped with electrical tape, placed in double-zip lock bags and air-tight Pyrex containers, and stored in hotel rooms until express courier shipping to Queen's University, where they were stored in the lab with a measured GEM concentration of  $\approx 2$  ng m<sup>-3</sup> (essentially background levels) until analysis. A total of five field blanks (transported to site, opened and immediately closed, and stored in sealed Pyrex containers) were utilized across the experiments and the mean total Hg (THg) concentration (1.63 ± 0.47 ng g<sup>-1</sup>) was used to blank correct all MerPAS samples as previously described (McLagan et al., 2016).

Crop Samples: Due to the developmental stage of the plants at the control farm, cassava and maize samples couldn't be replicated, and the maize kernel was unavailable for analysis. After plant sampling, plants were segmented into different tissue samples with a sharpened, pre-(soap) washed, DI water rinsed stainless knife then transported to the University of Lagos the day after sampling (at ambient temperature) then refrigerated for two days at 4 °C before oven drying after arrival. Crop samples (with the exception of tubers/grains) were then rinsed with deionized water, and oven-dried until constant weight 35-40 °C at the University of Lagos. Peanut nuts were removed from their husks (husks discarded); maize grains (kernels) were cut away from the ears (ears discarded); cassava tubers were peeled with a stainless-steel knife (peels discarded) and the tubers diced into cubes (≈1 cm³). The grains/tubers were rinsed, stored in double Ziplock bags, and oven-dried before shipping to Queen's University. Before analyses, foliage, stem, and root samples were chopped into fine pieces using (washed and rinsed) sharpened stainless sheers, while grains/tubers were crushed and ground in a ceramic mortar (washed and rinsed); all samples were thoroughly homogenized before removal of aliquots for analysis. Due to the earlier developmental stage of the plants at (control) Farm2, cassava and maize samples could not be replicated and maize kernel could not be sampled.



Figure S4: Farm1 sampling site (farmers harvesting peanuts).

# S3. Analytical Methods and Recoveries for CRMs

THg for soil and plant material: 0.01 - 0.2 g Aliquots of all soil and plant samples are weighed directly on pre-cleaned (scrubbed clean with surfactant and water, DI water rinsed, and baked at 450 °C in a furnace for a minimum of 30minutes) ceramic boats for analysis. An inorganic Hg stock solution in 5% nitric acid (Sigma Aldrich) was used for calibration of the MA-3000 (Nippon Instruments) and internal standard precision and recovery testing (see Section S3 for details). The temperature ramp for soil and crop samples was 200 °C for 60 seconds, a 60 second ramp to 800 °C, and held at 800 °C for 180 seconds in a 0.1 L/min flow rate of  $O_2$  (purity: 99.5 %).

MerPAS: To prevent issues of uncertainty associated with the heterogeneous distribution of Hg within the sulphur-impregnated activated carbon (HGR-AC; Calgon Carbon Corp.), the entire HGR-AC sorbent from each sampler was weighed and then analyzed in full, with the exception of the MerPAS from PS due to the very high concentrations measured. The HGR-AC from the PS MerPAS was weighed and then five to seven 0.01-0.02 g aliquots of the PS MerPAS were analysed and the mean concentration of these aliquots was used to generate the total mass of Hg (ng) sorbed to each sampler. While this adds some uncertainty, it prevents the MA-3000 being overwhelmed by Hg, which can have major impacts on analytical results; the very high concentrations also reduce the need for ultra-high precision (McLagan et al., 2019). ≈0.1 g of sodium carbonate, (pre-baked at 450 °C to remove any residual Hg) were also added onto the boats with HGR-AC to extend MA-3000 catalyst lifetimes (McLagan et al., 2017). The combustion method was altered to 60 seconds initial decomposition at 200 °C and a second ramp to a lower decomposition (or rather desorption) temperature of 400 °C, which was then held for 300 seconds. We hypothesize that this lower combustion/desorption temperature will reduce the production of catalyst poisoning sulphur-oxides and the "melting" of sodium carbonate and HGR-AC, which can impact internal components of the instrument. To ensure full recovery of Hg with this method 10 sample aliquots (unused HGR-AC from PS MerPAS) were run with this method and then the same aliquot was re-run with a decomposition temperature of 750°C, and the Hg signal in the follow up analyses at 750 °C did not differ from that of boat blanks (no sample). We recommend all future MerPAS users utilize the 400 °C Hg desorption method. GEM concentrations were calculated by dividing the blank corrected Hg mass (ng) in each sampler by the product of the deployment time (days) and the sampling rate (SR, m<sup>3</sup> day<sup>-1</sup>) (McLagan et al., 2016). For this study, GEM concentrations were based on a SR of 0.111 m<sup>3</sup> day<sup>-1</sup>, as recommended by Tekran Inc. for commercially distributed MerPAS (Tekran Instrument Corporation, n.d.). The SR was not adjusted for temperature or wind speed in these deployments as there were no local weather station data available. Also, considering the large range of GEM concentrations observed, the small reduction in uncertainty that temperature and wind speed adjustments would have an insignificant impact on results.

PTD analyses: Samples undergo a gradual heating ramp of  $\approx 0.6$  °C per second with the desorption by-products (including GEM) connected to the Lumex 915M Zeeman Hg atomic absorption spectrometer (254 nm) for continuous signal detection throughout sample heating. The temperature-based signal desorption profiles were compared to the absorption curves of a series of Hg reference materials (Hg<sup>0</sup>, HgCl<sub>2</sub>, Hg<sub>2</sub>Cl<sub>2</sub> (calomel), cinnabar: α-HgS, meta-cinnabar: β-HgS, and Hg<sup>2+</sup>-sulphate: HgSO<sub>4</sub>) in SiO<sub>2</sub> matrix to infer the species or "fractions" of Hg present in the samples from Biester and Scholz (1996), Mashyanov et al. (2017), and McLagan et al. (2022).

Methylmercury (MeHg) analysis: All samples were first freeze dried before analysis. Soil, seed, root, leave, and tuber samples were all distilled, the weight taken for distillation varied between  $\sim 200-300$  mg, depending on the type of sample. Samples were placed in Teflon distillation vessels with  $0.2 \, \text{M} \, \text{CuSO}_4$ , 20% KCl, and 50%  $\, \text{H}_2 \, \text{SO}_4$ . Mass addition of soil reference material, IAEA-158A, was similar to soil samples (between 200-300 mg) and precise amounts of enriched  $\, \text{Me}^{198} \, \text{Hg} \,$  isotope as an internal standard were added. Distillation vessels were heated to  $\sim 230 \, ^{\circ} \, \text{C}$  for approximately 4 hours until 50 mL of distillate was obtained. Precise volume of distillate was mixed with MQ water, acetate buffer (pH stabilizer), and sodium tetraethylborate ( $\, \text{Et}_4 \, \text{BNa}_4 \,$ , ethylating agent) in a glass bubbler.  $\, \text{N}_2 \,$  tubing was attached to the inlet and a Tenax trap was attached to the outlet portion of the glass bubbler. The solution was mixed and allowed to equilibrate for the ethylation reaction to be completed before bubbling the solution with  $\, \text{N}_2 \,$  and then purging the Tenax trap directly with  $\, \text{N}_2 \,$ .

A wire coil was wrapped around the Tenax trap to thermally desorb its contents. The Tenax trap was fixed to an inlet tubing for argon gas and an outlet tubing leading to a gas chromatography column (GC), where temperature is kept between 98 – 105 °C. The release mechanism for the sample consisted of heating the Tenax trap and displacing the sample with pure argon gas, enabling the sample to travel into the GC column where it separated by boiling point and moved to the pyrolytic column inside the hyphenated Inductively Coupled Plasma Mass Spectrometry (ICP-MS) (7700x, Agilent). Here, the species was broken down to mercury vapor and other compounds, which are then detected by the cold vapor atomic fluorescence spectrometry (CVAFS). Quantification of each sample was obtained from corresponding peaks signaling individual mercury isotopes. Me<sup>202</sup>Hg is used to calculate ambient MeHg concentration due to it being the most naturally abundant mercury isotope.

**QA/QC for THg:** Hg certified RMs used for QAQC were loam soil (ERM-CC141; European Union Joint Research Centre), woody biomass (AR1946; Alpha Resources LLC), high-sulphur coal (MerPAS analyses at 400 °C; SRM AR3701; Alpha Resources LLC), cotton biomass (IAEA-V-9; International Atomic Energy

Agency), apple leaves (NIST1515; National Institute of Standards and Technologies (NIST), and pine needles (NIST 1575a; NIST).

Table S1: Recoveries of CRMs used for all THg analysis.

CRM	Recovery (%)	Certified range (%)	n
ERM-CC141	98 ± 11	80 - 120	29
AR1946	104 ± 30	79 - 121	17
AR3701	105 ± 10	94 - 106	10
IAEA-V-9	78 ± 4	67 - 133	26
NIST1515	98 ± 5	94 - 106	29
NIST1575a*	110 ± 13	79 - 121	16

<sup>\*</sup>Based off round robin data.

**QA/QC for MeHg**: Blanks, standard reference materials, and duplicates were applied in the distillation process to ensure quality assurance. Similarly, blanks, ambient mercury, and enriched isotope spikes were added to the sample run when using the ICP-MS to ensure quality control.

Table S2: Recovery for CRM used for MeHg analysis

SRM	Duplicate RSD	MDL
99 ± 5%	9.07%	0.012
n = 4	n = 1	

Note: Soil Reference Material (SRM) used was IAEA-158A with a recovery value of  $1.80 \times 10^{-3} \pm 0.26 \times 10^{-3}$  mg kg<sup>-1</sup>. MDL = method detection limit. RSD = relative standard deviation.

#### QA/QC for stable isotope analysis:

Table S3: MDF and MIF values for standards for isotope analysis and 2SD analytical uncertainties.

Sample Name	MDF MIF								
Name	δ <sup>199</sup> Hg (‰)	δ <sup>200</sup> Hg (‰)	δ <sup>201</sup> Hg (‰)	δ <sup>20</sup> 2Hg (‰)	δ <sup>204</sup> Hg (‰)	Δ <sup>199</sup> Hg (‰)	$\Delta^{200}$ Hg (‰)	$\Delta^{20_1}$ Hg (‰)	$\Delta^{204}$ Hg (‰)
UM-	-0.17	-0.31	-0.46	-0.55	-0.84	-0.04 ±	-0.03	-0.05 ±	-0.03
Almaden	± 0.06	± 0.13	± 0.15	± 0.19	± 0.31	0.08	± 0.07	0.05	± 0.06
ETH-	-0.31	0.72 ±	-1.14±	-1.45 ±	-2.21	0.05 ±	-0.01	-0.05 ±	-0.04
Fluka	± 0.10	0.13	0.31	0.18	± 0.40	0.07	± 0.05	0.19	± 0.18

#### Clarifications on Hg stable isotope analysis method (taken from interactive discussion in review):

From a strict scientific point of view, Blum and Johnson (2017) recommend use of Tl, but do not rigorously compare to the case of 'not using Tl'. From a more practical point of view, the Blum lab (and the reviewer's JSI lab) uses a Nu Instruments MC-ICPMS, which is an instrument known to be undergo large shifts in mass bias during a 24h session. Use of Tl helps correcting mass bias on the Nu and it is used in all Nu labs. We did our Hg isotope analyses in the Sonke lab on a Neptune MC-ICPMS, well known for its high stability of mass bias. Consequently, Tl is of little use on Neptune instruments. Note that both Blum and Sonke labs recommend sample matrix cleanup before analysis, which also helps avoiding matrix-induced mass bias

and this was performed on all samples in this current study. Finally, on a Nu machine, the 12 Faraday cups allow measuring all Hg and Tl isotopes simultaneously. On many Neptunes, the 9 cups are physically restricted in their movement and do not allow collection of 203Tl, 204Hg, and 205Tl simultaneously; the Sonke lab therefore privileges measurement of 204Hg over Tl isotopes. To our knowledge, we are not aware of the exclusion of Sonke lab data, or other Neptune data (analysed without Tl) from review or synthesis works. The numerous high profile studies from both labs attest to the data quality; see for example Jiskra et al. (2021) which is published in Nature and uses the same methods without Tl-mass bias correction.

# S4. Equations for Two endmember mixing model

#### Two endmember mixing model:

Equation S1

Where:  $\delta^{202}$ Hg<sub>tissue:i</sub>,  $\delta^{202}$ Hg<sub>foliage</sub>, and  $\delta^{202}$ Hg<sub>soil</sub> are the MDF values for crop tissue "i", foliage, and soil, respectively, and  $f_{soil:i}$  and  $f_{foliage:i}$  are the fraction of Hg in tissue "i" derived from soil and air/foliage endmembers. This assumes all Hg in foliage is derived from air (as suggested in the literature: i.e., Zhou et al., 2021) and that soil-to-root uptake imparts no MDF for which we have little-to-no data on. Fractionation factors of Hg translocation from roots to soil are relatively unknown except for the recent study by Yuan et al. (2022). As annual or bi-annual harvest crops, cassava, maize, and peanuts are all shallow rooting species (Kengkanna et al., 2019; Nyakudya and Stroosnijder, 2014; Jongrungklang et al., 2011), thus we have adjusted the mean  $\delta^{202}$ Hg value for Farm1 soils (-0.26 ± 0.44 ‰) for the  $\epsilon^{202}$ Hg (-0.35 ± 0.17 ‰) from soil to shallow root epidermis/cortex only (<150cm) from Yuan et al. (2022) to give  $\delta^{202}$ Hg value of -0.61 ± 0.61 % for the soil-root endmember. We caution that these data are for a single tree species native to China (Lichocarpus xylocarpus) and there may be physiological differences between this species and the crops targeted in this study that could cause different fractionation factors between soils and root epidermis/cortex. Nonetheless, these are the only available data and we deem this the most appropriate estimation available. An alternative explanation could be that all the difference in MDF we observed between soil and roots is attributable to the translocation from roots to soil (no transfer from foliage to roots). However, we do not deem this explanation appropriate due to the data presented Yuan et al. (2022) show small fractionation from soil to outer root tissues (epidermis/cortex) and their data showing large differences in MDF and THg concentration between outer root tissues (epidermis/cortex) and inner root tissues (vascular bundle/stele). In addition, data from Sun et al. (2019) showed little-to-no difference in MDF between soils and whole maize root (like us they did no root dissection).

# S5. Method for estimation of annual GEM/Hg(0) dry deposition rates to crops

#### **Annual Hg dry deposition rates:**

$$F_{Hg(0):AGB} = AGB * (f_{foliage} * [THg]_{foliage:ASGM}) + AGB * (f_{other} * [THg]_{other:ASGM})$$
$$- AGB * (f_{foliage} * [THg]_{foliage:BG}) - AGB * (f_{other} * [THg]_{other:control})$$

Equation S2

Where: AGB is above ground biomass per area (kg km<sup>-2</sup>),  $f_{foliage}$  is fraction of AGB made up of foliage,  $[THg]_{foliage:FARM1}$ ,  $[THg]_{other:FARM2}$ , and  $[THg]_{other:FARM2}$  are the measured THg concentrations in foliage at Farm1, mean of other above ground tissues at Farm1, foliage at Farm2 (control), mean of other above ground tissues at Farm2 (control). Crop-specific, dw, post-harvest aboveground biomass data was sourced from the literature (peanut: 1,301 kg ha<sup>-1</sup>, Oliveira et al., 2024; maize: 17,500 kg ha<sup>-1</sup>, Li et al., 2016; cassava: 34,877 kg ha<sup>-1</sup>, Silva et al., 2013). Adjustments were made for peanuts and maize ( $F_{Hg(0):AGB}$  \* 2) by accounting for their respective planting cycles, as both crops are typically planted twice per year in Nigeria, which would double their annual capacity to take up Hg (ICRISAT, 2015; Agricdemy, n.d.). Cassava, in contrast, is typically planted annually. These planting cycles are not fixed globally and are subjected to weather conditions, agriculture of the area, and other factors, and difference in these cycles is a source of uncertainty for upscaling fluxes. For calculating the % of foliage within the total aboveground biomass (AGB), we relied on estimates from Zhu et al. (2019), which suggest that maize leaves constitute  $\approx$ 30% of the total AGB, while peanuts and cassava foliage comprise approximately  $\approx$ 55 and 35% respectively. (Phengvilaysouk and Wanapat, 2008); we assume a 10% uncertainty on these values.

For cassava and peanuts, we took this further by adding the flux of Hg from foliage to below ground edible parts using Equation S3:

$$F_{Hg(0):Total} = F_{Hg(0):AGB} + BY * (f_{air/foliage} * [THg]_{tuber/nut:FARM1}) - BY * (f_{air/foliage} * [THg]_{tuber/nut:FARM2})$$

Equation S3

Where:  $F_{Hg(0):Total}$  is the total above and below ground Hg(0) flux to crops (g km<sup>-2</sup>),  $f_{air/foliage}$  is the fraction of Hg in tuber/nuts derived from air, BY is the tuber/nut yield (kg km<sup>-2</sup>), and  $[THg]_{foliage:FARM1}$  and  $[THg]_{foliage:FARM2}$  are the THg concentrations in tuber/nut at Farm1 and Farm2 (control), respectively. BY were taken from the literature and are reported on an annual basis and are therefore not adjusted for crop cycles. The mean BY for cassava and peanuts(groundnuts) in Nigeria from 2000-2023 is  $9.1\pm2.2\times10^5$  kg km<sup>-2</sup> and  $1.3\pm0.2\times10^5$  kg km<sup>-2</sup> (FAO, 2025). Fully propagated uncertainties are associated with each estimate of annual Hg flux into the crops. These data are presented in Table S4.

Table S4: Fraction contribution of foliage to total Hg flux to crops

Crop	Total Hg(0) deposition flux to crops (g kg <sup>-1</sup> km <sup>-2</sup> )	Hg(0) deposition flux to crop foliage only (g kg <sup>-1</sup> km <sup>-2</sup> )	Contribution of foliage to total Hg(0) flux to crops (%)		
Peanut	110±80	100±32	92		
Maize	690±130	620±110	90		
Cassava	1170±180	1070±90	92		

## S6. Method for estimation probable dietary intake values

To estimate MeHg and THg exposures (THg = inorganic Hg (IHg) + MeHg) intake from cassava, peanuts/groundnut, and maize consumption, we calculated probable daily intake (PDI) values of MeHg and THg for the general adult population in Nigeria according to the following equation adapted from Zhao et al. (2019):

$$PDI = C \times IR \times A/bw$$

Eq. S4

Where: PDI is given in  $\mu$ g kg<sup>-1</sup> day<sup>-1</sup>, or the  $\mu$ g of MeHg/THg consumed per kg of body weight (bw; mean body weight for Nigerian adults is 68.2 kg; Chinedu and Emiloju, 2014) per day, C is the measured MeHg or THg concentration ( $\mu$ g kg<sup>-1</sup>) from Farm1 crops (Table S9 and Table S10, respectively), IR is daily intake rate (kg d<sup>-1</sup>), (see Table S5) and A is the absorption rate of Hg by the human body, which is 7% for IHg and 95% for MeHg (WHO, 1990; Zhao et al., 2019). The IHg absorption rate is assumed for THg exposures due to the low MeHg fraction in all samples. The mean daily dietary intakes are summative and therefore we calculate the sum PDI values for MeHg and THg based on the mean consumption of each of these crops by Nigerians (Table S5).

Table S5: The average daily intake rate (IR) for each of the studied crops.

Crop	Mean daily Intake rate (kg day <sup>-1</sup> )	IHg absorption rate	MeHg absorption rate	PDI THg (µg kg¹ day¹)	PDI MeHg (µg kg <sup>-1</sup> day <sup>-1</sup> )	Reference for daily intake rate
Maize	0.066±0.007#	0.07±0.007	0.95±0.095#	0.00012±0.00084	0.00009±0.00035	Table 5 in Ezekiel et al. (2021)
Peanut/groundnut	0.052±0.005#	0.07±0.007	0.95±0.095#	0.0014±0.0011	NA	Table 5 in Ezekiel et al. (2021)
Cassava (tuber)	0.227±0.023#	0.07±0.007	0.95±0.095#	0.0048±0.0025	0.00031±0.00152	Philips et al. (2004)
**Cassava (leaves)	0.050±0.005#	0.07±0.007	0.95±0.095#	0.0164±0.0064	0.00063±0.00022	Table 1 in Latif and Müller (2015)
			Sum	0.023±0.007	0.0010±0.0016	

<sup>\*\* –</sup> Conservatively estimated at 50 g day<sup>-1</sup> based on available data from other African countries (Latif and Müller 2015). # – Uncertainty not provided, estimated at 10% of value.

# S7. THg and stable isotope full results for all samples

Table S6: Relevant data from GEM PAS deployments including final GEM concentrations (blank adjusted Hg for all samples was  $1.83 \pm 0.47$  ng and SR for all samples was 0.111 m<sup>3</sup>)

Sample	Mass of carbon	Mass of carbon	THg on carbon	Blank adjusted	Deployment	GEM	Longitude	Latitude
	sorbent (g)	sorbent measured (g)	sorbent (ng g <sup>-1</sup> )	sorbed Hg (ng)	Time (days)	(ng m <sup>-3</sup> )		
PS-GEM - 1	0.562	0.134	681	382	3.77	910	8.90264	7.70335
PS-GEM - 2	0.562	0.09	858	481	3.76	1200	8.90259	7.70356
PS-GEM - 3	0.562	0.263	1224	687	3.76	1600	8.90210	7.70362
F1-GEM - 1	0.522	0.522	26.2	12.4	2.83	39	8.90515	7.70176
F1-GEM - 2	0.529	0.529	34.2	17.0	2.83	54	8.90515	7.70176
F1-GEM - 3	0.546	0.291	22.1	10.5	2.82	33	8.90560	7.70168
F1-GEM - 4	0.545	0.248	28.6	14.0	2.82	45	8.90560	7.70168
F1-GEM - 5	0.553	0.553	43.6	22.4	2.81	72	8.90352	7.70196
F1-GEM - 6	0.546	0.429	49.2	25.2	2.81	81	8.90367	7.70173
F2-GEM	0.560	0.560	36.1	18.6	99.5	1.7	8.96564	7.67103
			Field Blank	S				
Travel Blank	0.539	0.294	1.44					
Field Blank F2a	0.550	0.267	1.78					
Field Blank F2b	0.550	0.275	1.52					
Field Blank F1	0.538	0.281	1.77					
Field Blank PS	0.530	0.285	2.62					
		Mean [THg]	1.83 ± 0.47					

Table S7: THg for Soil sample from the processing site. SD is for triplicated measurements, which was performed on all soil samples.

Sample	THg (µg kg <sup>-1</sup> )	SD
PS Soil S1	1580	420
PS Soil S2	2760	210
PS Soil S3	3930	1460
PS Soil S4	2510	160
PS Soil S5	557	6
PS Soil S6	2350	1430
PS Soil S7	535	210
PS Soil S8	2200	324
PS Soil S9	6540	1290
PS Soil S10	4010	250
PS Soil S11	1060	260
PS Soil S12	1540	540
PS Soil S13	2580	10
Mean PS Soils	2470	1640

Table S8: Soil THg concentrations for Farm1 and Farm2. SD is for triplicated measurements, which was performed on all soil samples. Only one sample of maize and cassava soils was obtained from Farm2 as we were only permitted to sample one plant of each of these species at Farm2.

Sample	Farm1 (µg kg <sup>-1</sup> )	Farm2 (µg kg <sup>-1</sup> )
Peanut soil 1	51.4 ± 2.0	4.43 ± 0.68
Peanut soil 2	33.3 ± 6.6	15.8 ± 2.8
Peanut soil 3	-	5.93 ± 0.26
Mean peanut soils	42.4 ± 12.8	8.71 ± 6.16
Maize soil 1	96.6 ± 61.0	23.3 ± 1.8
Maize soil 2	173 ± 8	
Maize soil 3	167 ± 7	ı
Mean maize soils	146 ± 31	23.3 ± 1.8
Cassava soil 1	23.2 ± 14.3	7.28 ± 1.23
Cassava soil 2	15.1 ± 0.7	1
Cassava soil 3	87.6 ± 17.4	-
Mean cassava soils	41.0 ± 39.7	7.28 ± 1.23
Combined farm soils	80.9 ± 62.1	11.3 ± 8.0

Table S9: THg in peanut, maize, and cassava tissues (foliage, stem, tuber/grain, and root) at Farm1 and Farm2 crops. SD is for triplicated measurements, which performed on all tissue samples. PN-N3, PN-F3 and MA-K3 were not recovered (lost) after drying at the University of Lagos.

Crop Species	Crop Tissue	Sample	Farm1: THg (µg kg <sup>-1</sup> )	Farm2: THg (µg kg <sup>-1</sup> )
Peanut (PN)	Foliage (F)	PN-F1	371 ± 6	10.2 ± 0.69
	Foliage	PN-F2	400 ± 211	5.12 ± 0.42
	Foliage	PN-F3	-	5.86 ± 0.36
	Foliage	PNF mean	385 ± 20	7.06 ± 2.74
	Stem (St)	PN-St1	19.0 ± 1.4	2.12 ± 0.52
	Stem	PN-St2	33.1 ± 6.8	2.31 ± 0.46
	Stem	PN-St3	14.0 ± 2.2	2.62 ± 0.58
	Stem	PN-St mean	22.1 ± 9.9	2.35 ± 0.25
	Nut (N)	PN-N1	11.2 ± 0.55	3.73 ± 2.52
	Nut	PN-N2	41.3 ± 1.21	_
	Nut	PN-N3	_	_
	Nut	PN-N mean	26.3 ± 21.3	3.73 ± 2.52
	Root (R)	PN-R1	69.0 ± 16.2	2.95 ± 0.60
	Root	PN-R2	84.5 ± 33.6	2.94 ± 0.67
	Root	PN-R3	96.4 ± 16.5	2.32 ± 0.61
	Root	PN-R mean	84.6 ± 14.1	2.74 ± 0.36
Maize (MA)	Foliage	MA-F1	223 ± 6	5.16 ± 0.40
IVIAIZE (IVIA)	Foliage	MA-F2	189 ± 2	3.10 ± 0.40
	Foliage	MA-F2	135 ± 2	_
		MA-F mean	133 ± 2 182 ± 44	5.16 ± 0.40
	Foliage		76.9 ± 2.5	
	Stem	MA-St1		0.65 ± 0.44
	Stem Stem	MA-St2 MA-St3	13.1 ± 3.0 5.20 ± 0.03	-
		+		0.65 + 0.44
	Stem	MA-St mean	31.7 ± 39.3	0.65 ± 0.44
	Kernel (K)	MA-K1	0.92 ± 0.26	-
	Kernel	MA-K2	2.64+0.69	-
	Kernel	MA-K3	2.64 ± 0.68	-
	Kernel	MA-K mean	1.78 ± 1.22	-
	Root	MA-R1	354 ± 39	5.74 ± 3.73
	Root	MA-R2	95.9 ± 22.0	-
	Root	MA-R3	154 ± 31	
	Root	MR mean	202 ± 136	5.74 ± 3.73
Cassava (CA)	Foliage	CA-F1	406 ± 11	13.2 ± 3.4
	Foliage	CA-F2	366 ± 4	-
	Foliage	CA-F2	188 ± 1	-
	Foliage	CA-F mean	320 ± 116	13.2 ± 3.36
	Stem	CA-St1	32.6 ± 5.6	2.55 ± 0.69
	Stem	CA-St2	22.4 ± 2.9	-
	Stem	CA-St3	21.2 ± 4.3	-
	Stem	CA-St mean	25.4 ± 6.3	2.55 ± 0.69
Tuber (	Tuber (T)	CA-T1	29.3 ± 2.6	1.68 ± 0.16
	Tuber	CA-T2	23.4 ± 2.1	-
	Tuber	CA-T3	8.98 ± 1.0	-
	Tuber	CA-T mean	20.5 ± 10.4	1.68 ± 0.16
	Root	CA-R1	123 ± 25	33.2 ± 17.0
	Root	CA-R2	58.4 ± 6.8	-
	Root	CA-R3	61.7 ± 7.7	-
	Root	CA-R mean	81.0 ± 36.3	33.2 ± 17.0

Table S10: MeHg concentration and % of THg in peanut, maize, and cassava tissues (foliage, stem, tuber/grain, and root) at Farm1 (stem were not included in MeHg analysis and maize kernel were not available for analysis). Maize foliage was duplicated with a relative standard deviation of 9%.

	Crop Tissue	MeHg (µg kg⁻¹)	MeHg % of THg
Peanut	Foliage	1.10	0.29
	Nut	0.12	0.48
	Root	0.23	0.35
	Soil	0.14	0.33
Maize	Foliage (duplicate1)	0.22	0.12
	Foliage (duplicate2)	0.25	0.14
	Root	0.29	0.15
	Soil	0.23	0.16
Cassava	Foliage	0.91	0.29
	Tuber	0.10	0.48
	Root	0.17	0.22
	Soil	0.12	0.29

Table S11: Isotope MDF for all Farm1 (and Farm2 air only) samples, "\*" marks replicated samples with 1SD values based on replicate variability (these 1 SD values are also italicised). PN represents peanuts, MA for maize, and CA for cassava. All isotope data for plant materials are from Farm1. Note that PS Soil a, b, and c is a mixture of S1 – S5, S6 – S11, and S12 – 13 respectively from Table S7.

Sample	Hg Trap	MDF									
Name	Recovery (%)	δ <sup>199</sup> Hg (‰)	2SD	δ <sup>200</sup> Hg (‰)	2SD	δ <sup>201</sup> Hg (‰)	2SD	δ <sup>202</sup> Hg (‰)	2SD	δ <sup>204</sup> Hg (‰)	2SD
PS Soil-a	91.1	-0.08	0.06	-0.19	0.13	-0.34	0.15	-0.39	0.19	-0.63	0.31
PS Soil-b	91.7	-0.10	0.06	-0.09	0.13	-0.20	0.15	-0.15	0.19	-0.23	0.31
PS Soil-c	82.0	0.14	0.06	0.69	0.13	0.92	0.15	1.42	0.19	2.16	0.31
Farm1 PN Soil	93.0	-0.20	0.06	-0.28	0.13	-0.48	0.15	-0.57	0.19	-0.90	0.31
Farm1 MA Soil	93.5	-0.08	0.06	0.03	0.13	0.01	0.15	0.05	0.19	0.09	0.31
PS-GEM-3	83.1	-0.58	0.06	-1.35	0.13	-2.02	0.15	-1.53	0.19	-4.00	0.31
PS-GEM-1	124.8	-0.55	0.06	-1.16	0.13	-1.76	0.15	-1.23	0.19	-3.53	0.31
GEM F1	83.3	-0.44	0.06	-1.07	0.13	-1.60	0.15	-0.94	0.19	-3.19	0.31
GEM F2	81.5	-0.41	0.06	-0.66	0.13	-0.93	0.15	-0.01	0.19	-1.62	0.31
PN Foliage	100	-0.92	0.06	-1.87	0.13	-2.85	0.15	-3.77	0.19	-5.62	0.31
MA Foliage*	97.4	-0.67	0.08	-1.27	0.16	-1.98	0.27	-2.51	0.32	-3.86	0.68
CA Foliage	99.9	-0.94	0.06	-1.90	0.13	-2.96	0.15	-3.83	0.19	-5.68	0.31
CA Stem	94	-0.87	0.06	-1.80	0.13	-2.77	0.15	-3.60	0.19	-5.46	0.31
PN Nuts*	120.9	-0.56	0.20	-1.27	0.28	-1.92	0.40	-2.54	0.51	-3.82	0.77
MA Kernel	124.2	-0.66	0.06	-1.50	0.13	-2.26	0.15	-2.94	0.19	-4.50	0.31
CA Tubers	90.5	-0.87	0.06	-1.89	0.13	-2.67	0.15	-3.65	0.19	-5.39	0.31
PN Roots	89.3	-0.52	0.06	-0.98	0.13	-1.45	0.15	-1.91	0.19	-2.99	0.31
MA Roots	88.5	-0.43	0.06	-0.76	0.13	-1.13	0.15	-1.51	0.19	-2.05	0.31
CA Roots	83.8	-0.40	0.06	-0.76	0.13	-1.07	0.15	-1.46	0.19	-2.17	0.31

Table S12: Isotope MIF for all Farm1 (and Farm2 air only) samples. PN represents peanuts, MA for maize, and CA for cassava. All isotope data for plant materials are from Farm1. Note that PS Soil a, b, and c is a mixture of S1 - S5, S6 - S11, and S12 - 13 respectively from Table S7.

Sample Name	Δ <sup>199</sup> Hg	2SD	Δ <sup>200</sup> Hg	2SD	Δ <sup>20</sup> 1Hg	2SD	Δ <sup>204</sup> Hg	2SD
	(‰)		(‰)		(‰)		(‰)	
PS Soil - a	0.02	0.08	0.00	0.07	-0.05	0.12	-0.05	0.18
PS Soil - b	-0.06	0.08	-0.02	0.07	-0.08	0.12	0.00	0.18
PS Soil - c	-0.21	0.08	-0.02	0.07	-0.15	0.12	0.04	0.18
F1 Soil	-0.05	0.08	0.01	0.07	-0.06	0.12	-0.06	0.18
F1 Soil	-0.09	0.08	0.01	0.07	-0.03	0.12	0.02	0.18
PS-GEM-3	0.09	0.08	-0.01	0.07	-0.01	0.12	0.00	0.18
PS-GEM-1	0.05	0.08	0.03	0.07	0.02	0.12	0.01	0.18
GEM F1	0.08	0.08	-0.02	0.07	-0.04	0.12	-0.07	0.18
GEM F2	-0.12	80.0	-0.08	0.07	-0.07	0.12	0.10	0.18
PN Foliage	0.03	0.08	0.02	0.07	-0.02	0.12	0.02	0.18
MA Foliage	-0.04	0.08	0.00	0.07	-0.09	0.12	-0.10	0.20
CA Foliage	0.02	0.08	0.02	0.07	-0.08	0.12	0.04	0.18
CA Stem	0.04	0.08	0.01	0.07	-0.07	0.12	-0.08	0.18
Nuts	0.08	0.08	0.01	0.02	-0.02	0.12	-0.02	0.18
Kernel	0.08	0.08	-0.02	0.07	-0.05	0.12	-0.11	0.18
Tuber	0.05	0.08	-0.05	0.07	0.08	0.12	0.08	0.18
PN Roots	-0.04	0.08	-0.02	0.07	-0.01	0.12	-0.13	0.18
MA Roots	-0.05	80.0	0.00	0.07	0.00	0.12	0.21	0.18
CA Roots	-0.04	0.08	-0.03	0.07	0.03	0.12	0.01	0.18

# S8. Pyrolytic Thermal Desorption (PTD) curves for Farm1 and Processing Site (PS) solid-phase speciation/fractionation analyses

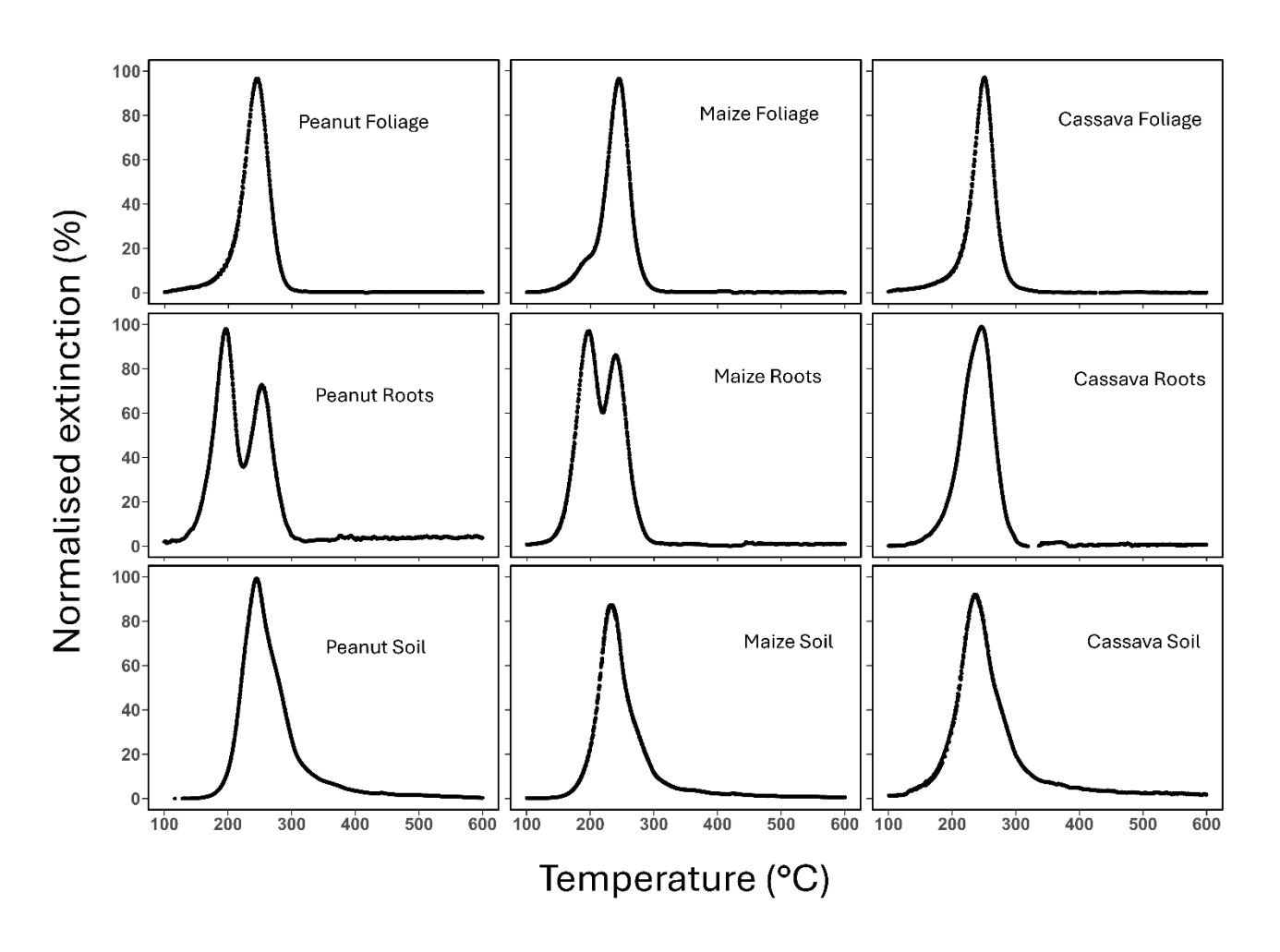


Figure S5: PTD curves for all Farm1 samples. Normalization method follow that described in McLagan et al. (2022).

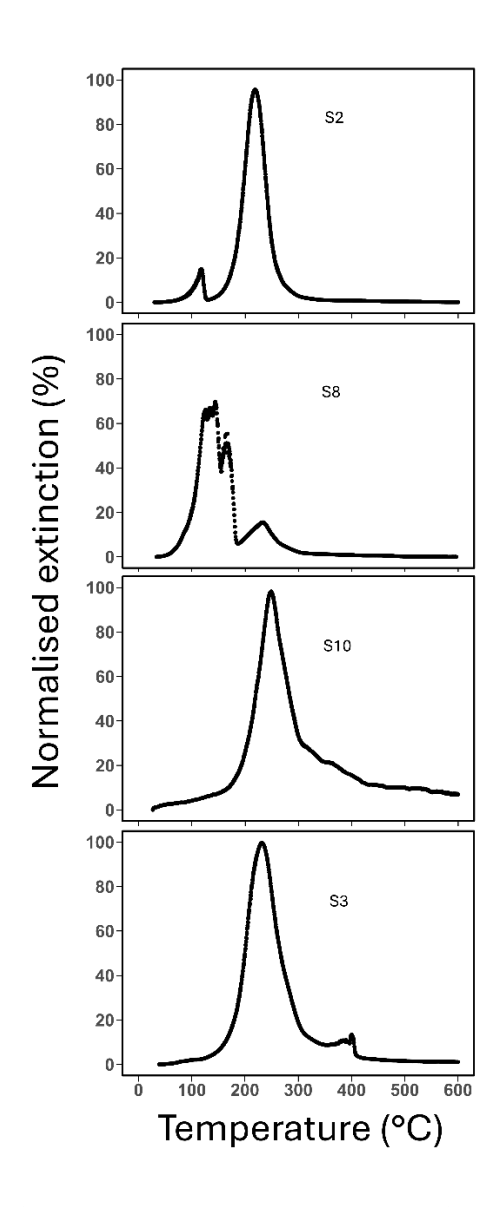


Figure S6: PTD curves for Processing site soil samples. Normalization method follow that described in McLagan et al. (2022).

## References (used in Supplementary Information)

Agricdemy: Maize Farming in Nigeria, https://agricdemy.com/post/maize-farming-nigeria, n.d.

Biester, H., and Scholz, C.: Determination of mercury binding forms in contaminated soils: mercury pyrolysis versus sequential extractions, Environmental science & technology, 31, 233-239, https://doi.org/10.1021/es960369h, 1996.

Chinedu, S. N., and Emiloju, O. C.: Underweight, overweight and obesity amongst young adults in Ota, Nigeria, Journal of Public Health and Epidemiology, 6, 235-238, https://doi.org/10.5897/JPHE2014.0638, 2014.

Davies, H. O.: Mercury Contamination Risk Assessment in Artisanal Small-Scale Gold Mining Sites in Uke and Environs, Nasarawa State, PhD thesis, Lead City University, https://repository.lcu.edu.ng/handle/123456789/526, 2023.

Ezekiel, C. N., Ayeni, K. I., Akinyemi, M. O., Sulyok, M., Oyedele, O. A., Babalola, D. A., Ogara, I. M., and Krska, R.: Dietary risk assessment and consumer awareness of mycotoxins among household consumers of cereals, nuts and legumes in north-central Nigeria, Toxins, 13, 635, https://doi.org/10.3390/toxins13090635, 2021.

FAO: Food and Agriculture Organization of the United Nations, Rome, ITA, https://www.fao.org/faostat/en/#data/QCL, 2025.

Hojdová, M., Rohovec, J., Chrastný, V., Penížek, V., and Navrátil, T.: The influence of sample drying procedures on mercury concentrations analyzed in soils, Bulletin of environmental contamination and toxicology, 94, 570-576, https://doi.org/10.1007/s00128-015-1521-9, 2015.

ICRISAT: Groundnut Production in Nigeria, International Crops Research Institute for the Semi-Arid Tropics, Federal Ministry of Agriculture and Rural Development, https://oar.icrisat.org/8856/1/2015-084%20Gnut%20Production%20in%20Nigeria.pdf, 2015.

Iorhemba, A., and Mijinyawa, Y.: Development of Wind Rosettes for Farmstead Planning and Layout in North Central Nigeria, International Journal of Advances in Engineering and Management, 3, 671-679, https://ijaem.net/issue\_dcp/Development%20of%20Wind%20Rosettes%20for%20Farmstead%20Planning%20and%20Layout%20in%20North%20Central%20Nigeria.pdf, 2021.

Jiskra, M., Heimbürger-Boavida, L.E., Desgranges, M.M., Petrova, M.V., Dufour, A., Ferreira-Araujo, B., Masbou, J., Chmeleff, J., Thyssen, M., Point, D. and Sonke, J.E.: Mercury stable isotopes constrain atmospheric sources to the ocean. *Nature*, 597(7878), 678-682. https://doi.org/10.1038/s41586-021-03859-8, 2021.

Jongrungklang, N., Toomsan, B., Vorasoot, N., Jogloy, S., Boote, K. J., Hoogenboom, G., and Patanothai, A.: Rooting traits of peanut genotypes with different yield responses to pre-flowering drought stress, Field Crops Research, 120, 262-270, https://doi.org/10.1016/j.fcr.2010.10.008, 2011.

Kengkanna, J., Jakaew, P., Amawan, S., Busener, N., Bucksch, A., and Saengwilai, P.: Phenotypic variation of cassava root traits and their responses to drought, Applications in plant sciences, 7, e01238, https://doi.org/10.1002/aps3.1238, 2019.

Latif, S., and Müller, J.: Potential of cassava leaves in human nutrition: A review, Trends in Food Science & Technology, 44, 147-158, https://doi.org/10.1016/j.tifs.2015.04.006, 2015.

Li, W., Niu, Z., Chen, H., Li, D., Wu, M., and Zhao, W.: Remote estimation of canopy height and aboveground biomass of maize using high-resolution stereo images from a low-cost unmanned aerial vehicle system, Ecological indicators, 67, 637-648, https://doi.org/10.1016/j.ecolind.2016.03.036, 2016.

McLagan, D. S., Mitchell, C. P., Huang, H., Lei, Y. D., Cole, A. S., Steffen, A., Hung, H., and Wania, F.: A high-precision passive air sampler for gaseous mercury, Environmental Science & Technology Letters, 3, 24-29, https://doi.org/10.1021/acs.estlett.5b00319, 2016.

McLagan, D. S., Monaci, F., Huang, H., Lei, Y. D., Mitchell, C. P., and Wania, F.: Characterization and quantification of atmospheric mercury sources using passive air samplers, Journal of Geophysical Research: Atmospheres, 124, 2351-2362, https://doi.org/10.1029/2018JD029373, 2019.

McLagan, D. S., Mitchell, C. P., Huang, H., Abdul Hussain, B., Lei, Y. D., and Wania, F.: The effects of meteorological parameters and diffusive barrier reuse on the sampling rate of a passive air sampler for gaseous mercury, Atmospheric Measurement Techniques, 10, 3651-3660, https://doi.org/10.5194/amt-10-3651-2017, 2017.

McLagan, D. S., Schwab, L., Wiederhold, J. G., Chen, L., Pietrucha, J., Kraemer, S. M., and Biester, H.: Demystifying mercury geochemistry in contaminated soil–groundwater systems with complementary mercury stable isotope, concentration, and speciation analyses, Environmental Science: Processes & Impacts, 24, 1406-1429, https://doi.org/10.1039/D1EM00368B, 2022.

Misganaw, C. D., and Bayou, W. D.: Tuber yield and yield component performance of cassava (Manihot esculenta) varieties in Fafen District, Ethiopia, International Journal of Agronomy, 2020, 5836452, https://doi.org/10.1155/2020/5836452, 2020.

Mashyanov, N. R., Pogarev, S. E., Panova, E. G., Panichev, N., and Ryzhov, V.: Determination of mercury thermospecies in coal, Fuel, 203, 973-980, https://doi.org/10.1016/j.fuel.2017.03.085, 2017.

Nyakudya, I. W., and Stroosnijder, L.: Effect of rooting depth, plant density and planting date on maize (Zea mays L.) yield and water use efficiency in semi-arid Zimbabwe: Modelling with AquaCrop, Agricultural Water Management, 146, 280-296, https://doi.org/10.1016/j.agwat.2014.08.024, 2014.

Odukoya, A. M., Uruowhe, B., Watts, M. J., Hamilton, E. M., Marriott, A. L., Alo, B., and Anene, N. C.: Assessment of bioaccessibility and health risk of mercury within soil of artisanal gold mine sites, Niger, North-central part of Nigeria, https://doi.org/10.1007/s10653-021-00991-2, 2022.

Oliveira, M. F., Carneiro, F. M., Ortiz, B. V., Thurmond, M., Oliveira, L. P., Bao, Y., Sanz-Saez, A., and Tedesco, D.: Predicting below and above-ground peanut biomass and maturity using multi-target regression, Computers and Electronics in Agriculture, 218, 108647, https://doi.org/10.1016/j.compag.2024.108647, 2024.

Phengvilaysouk, A., and Wanapat, M.: Study on the effect of harvesting frequency on cassava foliage for cassava hay production and its nutritive value, Livestock Research for Rural Development, 20, http://www.lrrd.org/lrrd20/supplement/amma1.htm, 2008.

Phillips, T. P., Taylor, D. S., Sanni, L. O., and Akoroda, M. O.: A cassava industrial revolution in Nigeria: The potential of a new industrial crop, https://www.fao.org/4/y5548e/y5548e00.pdf, 2004.

Reis, A. T., Coelho, J. P., Rucandio, I., Davidson, C. M., Duarte, A. C., and Pereira, E.: Thermo-desorption: a valid tool for mercury speciation in soils and sediments?, Geoderma, 237, 98-104, https://doi.org/10.1016/j.geoderma.2014.08.019, 2015.

Silva, T. S., Silva, P. S. L., Braga, J. D., da Silveira, L. M., and de Sousa, R. P.: Planting density and yield of cassava roots, Revista Ciência Agronômica, 44, 317–324, https://doi.org/10.1590/S1806-66902013000200014, 2013.

Sun, G., Feng, X., Yin, R., Zhao, H., Zhang, L., Sommar, J., Li, Z., and Zhang, H.: Corn (Zea mays L.): A low methylmercury staple cereal source and an important biospheric sink of atmospheric mercury, and health risk assessment, Environment international, 131, 104971, https://doi.org/10.1016/j.envint.2019.104971, 2019.

WHO: Environmental health criteria 101: Methylmercury, World Health Organization, Geneva, CHE, https://apps.who.int/iris/bitstream/handle/10665/38082/9241571012\_eng.pdf, 1990.

Yoshimura, A., Koyo, S., and Veiga, M. M.: Estimation of mercury losses and gold production by Artisanal and Small-Scale Gold Mining (ASGM), Journal of Sustainable Metallurgy, 7, 1045–1059, https://doi.org/10.1007/s40831-021-00394-8, 2021.

Yuan, W., Wang, X., Lin, C. J., Wu, F., Luo, K., Zhang, H., Lu, Z., and Feng, X.: Mercury uptake, accumulation, and translocation in roots of subtropical forest: implications of global mercury budget, Environmental Science & Technology, 56, 14154-14165, https://doi.org/10.1021/acs.est.2c04217, 2022.

Zhao, H., Yan, H., Zhang, L., Sun, G., Li, P., and Feng, X.: Mercury contents in rice and potential health risks across China, Environ. Int., 126, 406-412, https://doi.org/10.1016/j.envint.2019.02.055, 2019.

Zhu, Y., Zhao, C., Yang, H., Yang, G., Han, L., Li, Z., Feng, H., Xu, B., Wu, J., and Lei, L.: Estimation of maize above-ground biomass based on stem-leaf separation strategy integrated with LiDAR and optical remote sensing data, PeerJ, 7, e7593, https://doi.org/10.7717/peerj.7593, 2019.